

# Optical absorptivity of $\text{La}_{1.87}\text{Sr}_{0.13}\text{CuO}_4$ below the superconducting plasma edge

J. T. Birmingham,\* S. M. Grannan,<sup>†</sup> and P. L. Richards

*Department of Physics, University of California, and Materials Sciences Division, Lawrence Berkeley Laboratory, Berkeley, California 94720*

J. Kircher, M. Cardona, and A. Wittlin<sup>‡</sup>

*Max-Planck-Institut für Festkörperforschung, Heisenbergstraße 1, D-70569 Stuttgart, Germany*

(Received 9 July 1998)

We have directly measured the far-infrared absorptivity of single crystal  $\text{La}_{1.87}\text{Sr}_{0.13}\text{CuO}_4$  at 2 K for radiation between 6 and  $420\text{ cm}^{-1}$  polarized along the  $c$  axis. We have computed the dielectric functions  $\epsilon^c(\omega)$  and conductivity  $\sigma^c(\omega)$  using a Kramers-Kronig analysis. The existence of nonzero losses below the plasma edge and down to the lowest frequency measured is consistent with a model of a superconducting gap with nodes. From the calculation of  $\epsilon^c(\omega)$ , we deduce a value of  $230 \pm 10\text{ cm}^{-1}$  for the unscreened plasma frequency in the superconducting state. A small peak in the  $\sigma_1^c(\omega)$  is seen near  $10\text{ cm}^{-1}$ . [S0163-1829(99)04701-3]

## I. INTRODUCTION

The far-infrared conductivity  $\sigma^c(\omega)$  in the direction perpendicular to the  $\text{CuO}_2$  planes of the  $\text{La}_{2-x}\text{Sr}_x\text{CuO}_4$  (214) family of high- $T_c$  superconductors depends both on the normal state conductivity and on the symmetry of the superconducting gap. Neither is well understood at present, especially in compounds that are less than optimally doped. Two models have been proposed to describe this normal-state conductivity. One scenario, put forward by Anderson and collaborators, postulates the absence of any coherent transport of carriers along the  $c$  axis in the normal state.<sup>1</sup> In this picture, strong electronic correlations decouple the spin and charge degrees of freedom of the carriers, and, as a consequence, the carriers are “confined” to the  $\text{CuO}_2$  planes. The optical response  $\sigma^c(\omega)$  resembles that of an ionic insulator, and there is little or no spectral weight at far-infrared frequencies. As the compound is cooled, the tendency of the system to lower its kinetic energy, and thus overcome the “confinement,” drives the superconducting transition and the corresponding condensation of Cooper pairs. Josephson tunneling of Cooper pairs restores coherent transport in the superconducting state. This model predicts that the superconducting transition is accompanied by the appearance of a distinct plasma edge in the optical response corresponding to collective excitations of charge pairs. In the second, very different scenario, the material is a bad but fairly conventional metal, with an extremely anisotropic mass and scattering rate for the free carriers.<sup>2</sup> In this picture the change in the optical spectrum induced by superconductivity is explained by the temperature dependences of both the density of superconducting pairs and the scattering rate of normal-state carriers. The differences between the far-infrared responses predicted by the two models are subtle.<sup>3</sup>

Optical measurements on 214 materials have been made since the early days of high- $T_c$  superconductivity<sup>4</sup> and have recently generated renewed interest. Initially, polycrystalline films were studied and a reflectivity edge was observed near  $50\text{ cm}^{-1}$  for temperatures below  $T_c$ .<sup>5-9</sup> More recently, single crystals have become available, and the  $c$ -axis optical re-

sponse has been measured separately from the in-plane optical response.<sup>2,10,11,12</sup> Above  $T_c$ , the far-infrared reflectivity along the  $c$  axis is typical of a doped insulator, with strong phonon peaks seen on top of an electronic background. While there is no disagreement about the position of the peaks,<sup>13</sup> the interpretation of the continuum between them remains in dispute. Kim *et al.* point<sup>11</sup> to signatures of incoherent transport above  $T_c$ , i.e., a Drude liquid with an extremely high scattering rate and plasma frequency (“dirty” limit parametrization.) However, Tamasaku *et al.*,<sup>2</sup> and later Henn *et al.*,<sup>12</sup> interpret very similar data using a Drude model with a small scattering rate and plasma frequency (parametrization approaching the “clean” limit.)

Below  $T_c$  the optical response is dominated by the plasma edge. The  $c$ -axis absorptivity in 214 materials is much larger than the in-plane absorptivity, and hence the plasma edge dominated the loss seen in the early investigations using the polycrystalline samples. The single crystal reflectivity experiments from several groups at frequencies above the plasma edge are in qualitative agreement with each other, at least at temperatures well below  $T_c$ .<sup>2,10,11,12</sup> Below the edge, the reflectivity is difficult to determine because the absorptivity becomes smaller than the  $\sim 1\%$  accuracy of typical reflectivity measurements. In addition, far-infrared measurements become increasingly difficult in general as the frequency is reduced. Although in-plane studies of the optical response have been recently extended to mm wavelengths,<sup>14</sup> relatively little is known about the details of the out-of-plane response. Optical measurements at low temperature with both  $\hbar\omega$  and  $kT \ll kT_c$  probe the absorptivity below the superconducting gap energy and hence should contribute to the investigation of the symmetry of the order parameter. Such studies may also shed some light on the dynamics of Josephson plasma excitations in 214 compounds, in particular on the issue of the longitudinal versus transverse excitation of the Josephson plasmons in small crystals.<sup>15</sup>

In this paper we extend the existing optical data of  $\sigma^c(\omega)$  for  $\text{La}_{1.87}\text{Sr}_{0.13}\text{CuO}_4$  to lower temperatures and lower frequencies by directly measuring the far-infrared absorptivity of a single crystal ( $T_c = 31\text{ K}$ ) between 6 and  $420\text{ cm}^{-1}$  for

radiation with the electric field polarized along the  $c$  axis at 2 K. These measurements complement ellipsometric reflectivity measurements<sup>12</sup> made on the same sample between 35 and 700  $\text{cm}^{-1}$  at 10 K. We have found that there is significant absorption at 2 K at frequencies down to 10  $\text{cm}^{-1}$ . Moreover, there is structure in the absorptivity at frequencies below the plasma edge. Our ability to determine the mechanism for the small losses at frequencies below the plasma edge is limited by questions of sample quality. We note that nominally identical crystals<sup>10</sup> have been measured that have narrower phonon linewidths and lower overall electronic background conductivities than the one used in this study. A preliminary report of our early results has appeared previously.<sup>16</sup>

## II. EXPERIMENT

The  $\text{La}_{1.87}\text{Sr}_{0.13}\text{CuO}_4$  single crystal measured was grown at the University of Amsterdam by the traveling-solvent floating-zone method.<sup>17</sup> The material grew as a cylindrical crystal (7 mm diameter and several cm in length), with the  $c$  axis oriented along one diameter. A  $\sim 1$  mm thick semicircular slice was cut from the large crystal for use in the absorptivity measurements. The (100) surfaces of the sample were mechanically polished, and the orientation of the axes was determined by Raman scattering and Laue x-ray diffraction.<sup>12</sup> The sample had a  $T_c$  of 31 K as measured by transport and magnetization measurements. Details of the sample characterization can be found elsewhere.<sup>12,18</sup>

We used the  $\text{La}_{1.87}\text{Sr}_{0.13}\text{CuO}_4$  crystal as the absorbing element in a composite bolometric far-infrared detector<sup>19,20</sup> in conjunction with a step-scanned Michelson Fourier spectrometer to directly measure its optical absorptivity. We determined the absorptivity of the  $\text{La}_{1.87}\text{Sr}_{0.13}\text{CuO}_4$  by comparing the detector response with that of another bolometer with a well-characterized gold absorber. The cryogenic portion of the apparatus was built by Miller *et al.*,<sup>21</sup> and is shown schematically in Fig. 1. Chopped infrared radiation from the spectrometer passes through a light pipe and both warm and cold low-pass filters and is split approximately symmetrically by a roof mirror into two beams. The cold filter is chosen to minimize background optical loading that limits detector sensitivity. A 15  $\mu\text{m}$  thick black polyethylene filter is used for the high frequency measurements; a 50  $\mu\text{m}$  thick MIR-X filter<sup>22</sup> is used for frequencies between 20 and 50  $\text{cm}^{-1}$ , and a 1 mm thick Fluorogold<sup>23</sup> filter is used for frequencies below 20  $\text{cm}^{-1}$ . One beam passes through a grid polarizer<sup>24</sup> with a 3.6  $\mu\text{m}$  grid period to the superconducting sample bolometer; the other beam is directed to a reference bolometer with a well-characterized gold film sputtered on sapphire as the absorbing element. The crystal was suspended in vacuum by nylon threads, with a small neutron-transmutation-doped (NTD) Ge thermistor<sup>25</sup> and a NiCr heater glued to its back side. The time constant  $\tau = C/G$  of the bolometer is determined by the heat capacity  $C$  of the crystal and the attachments to it and by the thermal conductance  $G$  of the electrical leads which connect the  $\sim 2$  K thermistor to the heat sink at  $\sim 1.5$  K. The effects of asymmetry in the two optical paths are discussed below.

We measured the responses of the  $\text{La}_{1.87}\text{Sr}_{0.13}\text{CuO}_4$  and gold reference bolometers with a lock-in amplifier synchro-

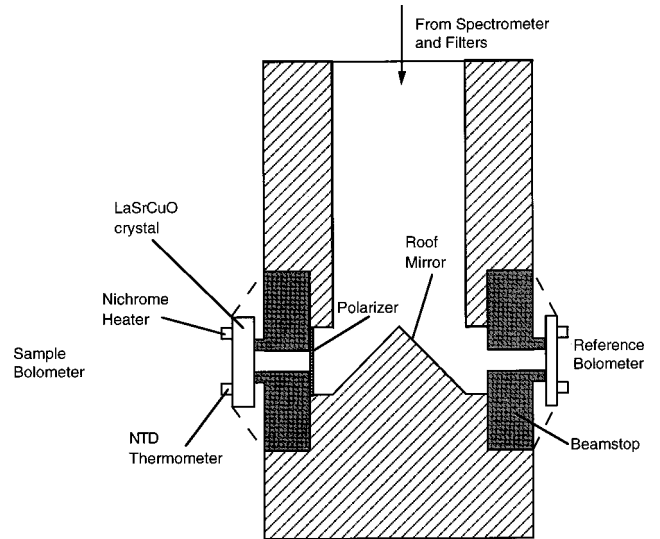


FIG. 1. Cryogenic portion of the experimental apparatus. Chopped radiation from the spectrometer is split symmetrically by the roof mirror and directed through beamstops toward the sample and reference bolometers.

nized with the chopper. The measured output spectrum from the sample detector can be expressed as

$$F_s(\omega) = L_s(\omega)T(\omega)A_s(\omega)S_s(f), \quad (1)$$

where  $L_s(\omega)$  is the infrared spectrum incident on the sample bolometer,  $T(\omega)$  is the transmittance of the polarizer,  $A_s(\omega)$  is the absorptivity of the sample, and  $S_s(f)$  is the responsivity of the sample detector to absorbed optical power chopped at the frequency  $f = 7$  Hz. The output spectrum from the reference detector is given by a similar expression,  $F_r(\omega) = L_r(\omega)A_r(\omega)S_r(f)$ , where the polarizer transmittance  $T(\omega)$  has been replaced by unity. If we assume that the spectrum reflected off each side of the roof mirror  $L(\omega)$  is the same for each bolometer, the absorptivity of the superconducting sample can be determined from the measured output spectra and the responsivities of the two bolometers:

$$A_s(\omega) = \frac{F_s(\omega)S_r(f)A_r(\omega)}{F_r(\omega)S_s(f)T(\omega)}. \quad (2)$$

The absorptivity  $A_r(\omega)$  of the gold reference film is well described<sup>21</sup> by the classical skin effect with  $n = 3.6 \times 10^{22} \text{ cm}^{-3}$  and  $\rho = 5.9 \mu\Omega \text{ cm}$ . The polarizer transmittance  $T(\omega)$  was directly measured and is shown in Fig. 2 of Ref. 24. At 50  $\text{cm}^{-1}$ , the transmittance is close to the ideal value of 0.5 but falls to 0.35 at higher frequencies, primarily because of reflection and absorption by the Mylar substrate. The transmittance of crossed polarizers varies from 2 to 6 % over the frequency range of our measurement. Thus, the polarizer leakage does not significantly affect our  $c$ -axis results.

The responsivities of the two bolometers to absorbed optical power were obtained from a combination of electrical and optical measurements. We dissipated electrical power at 7 Hz in NiCr heaters attached to the bolometers and measured the responses of the Ge thermistors to determine the electrical responsivities at this frequency. We then measured the frequency dependence of the response of each bolometer to chopped optical and electrical power and confirmed that

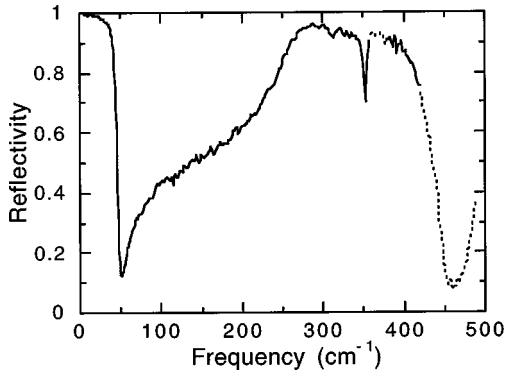


FIG. 2. Reflectivity along the  $c$  axis of a  $\text{La}_{1.87}\text{Sr}_{0.13}\text{CuO}_4$  crystal deduced from absorptivity measurements at 2 K (solid curve) and ellipsometric measurements (Ref. 12) at 10 K (dotted curve).

they were identical. Thus, the same simple thermal circuits could be used to model the devices for both optical and electrical loading, and the electrical responsivities could be equated with the responsivities to absorbed optical power.

Our measurements are affected by the following errors. We measured  $L(\omega)$  to be the same for each bolometer within 5%, differing only by a multiplicative factor independent of  $\omega$  that arises from asymmetry in the two optical paths. The responsivities  $S_r(f)$  and  $S_s(f)$  are also independent of  $\omega$  and were measured to better than 10% accuracy. The polarizer transmittance  $T(\omega)$  introduces a frequency-dependent error of less than 3%. The signal-to-noise ratios of the output spectra  $F_r(\omega)$  and  $F_s(\omega)$  are about 100 for all but the lowest frequencies measured. After accounting for the abovementioned factors, the absorptivity is known to within a scaling factor of approximately 15%, while the shape is known to a few percent. If the sample reflectivity is 99%, for example, the conservative estimate of 15% error in the absolute value of the absorptivity translates into an error of 0.15% in the reflectivity, much better than what can be directly obtained from reflectivity measurements. The uncertainty becomes significantly larger for frequencies below  $15 \text{ cm}^{-1}$ . At high frequencies where the reflectivity is small, the advantage of absorptivity measurements disappears.

### III. ABSORPTIVITY MEASUREMENTS

In Fig. 2 we plot the  $c$ -axis reflectivity  $R^c$  (solid curve) of the  $\text{La}_{1.87}\text{Sr}_{0.13}\text{CuO}_4$  crystal at 2 K between 6 and  $420 \text{ cm}^{-1}$  calculated from a measurement of the absorptivity  $A^c$ . Because the sample is sufficiently thick, there is no transmitted light, and  $R^c = 1 - A^c$ . The optical phonons<sup>12</sup> at 312 and  $352 \text{ cm}^{-1}$  are clearly seen. We have replaced and augmented the data between 358–381 and 419–489  $\text{cm}^{-1}$  with the reflectivity calculated from ellipsometric measurements<sup>12</sup> made on the same sample. In these regions of low polarizer transmittance (dotted curve) we believe the ellipsometric measurements to be more trustworthy than our absorptivity data.

In Fig. 3 we show the effect of a 10% absorptivity scaling error on the derived reflectivity. The solid curve shows the measured data from Fig. 2. The dotted and dashed curves correspond to multiplying the absorptivity by 0.9 and 1.1, respectively.

In Fig. 4 we compare our results with reflectivity

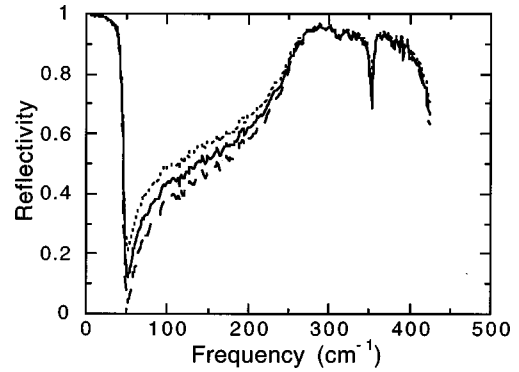


FIG. 3. Reflectivity at 2 K along the  $c$  axis of a  $\text{La}_{1.87}\text{Sr}_{0.13}\text{CuO}_4$  crystal deduced from absorptivity measurements (solid curve) and from absorptivity data multiplied by 0.9 (dotted curve) and 1.1 (dashed curve).

measurements<sup>11,12</sup> from two groups. The reflectivity derived from our absorptivity measurement is shown as a solid curve. We have not included the polarizer correction between 358 and  $381 \text{ cm}^{-1}$ . The reflectivity shown as a dotted curve was measured by ellipsometry on a mosaic sample, one crystal of which we used for our absorptivity measurements, and was used to support the clean limit scenario. The other (dashed curve) was measured on a  $\text{La}_{1.85}\text{Sr}_{0.15}\text{CuO}_4$  sample from the same grower and was used to support the dirty limit scenario. All three curves agree qualitatively. In the frequency range where we expect the largest systematic errors in our measurement, the differences between the curves agree within the experimental noise (see Fig. 3). In the reststrahlen band, where the smallest error for our experiment is expected, the two curves that have been measured on the same sample agree better with each other than with the third curve. This comparison shows that sample issues are still important, even though sample preparation techniques have reached considerable maturity. The higher reflectivity in the reststrahlen region measured in the sample used in our study is evidence that it is of higher quality than the other sample.

The steep fall of reflectivity at approximately  $41 \text{ cm}^{-1}$ , which is identified as the screened Josephson plasma fre-

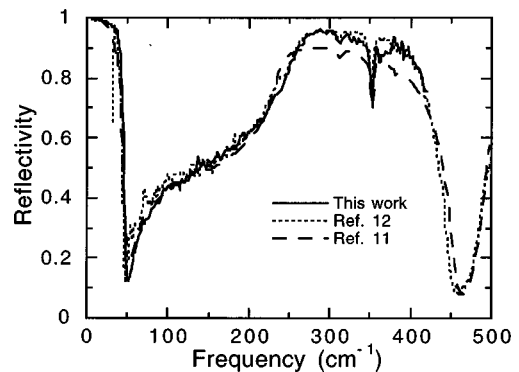


FIG. 4. Reflectivity along the  $c$  axis of a  $\text{La}_{1.87}\text{Sr}_{0.13}\text{CuO}_4$  crystal deduced from absorptivity measurements (solid curve), from ellipsometric measurements (Ref. 12) on a mosaic sample that included the crystal used in this work (dotted curve), and from measurements (Ref. 11) on a  $\text{La}_{1.85}\text{Sr}_{0.15}\text{CuO}_4$  sample from the same grower (dashed curve).

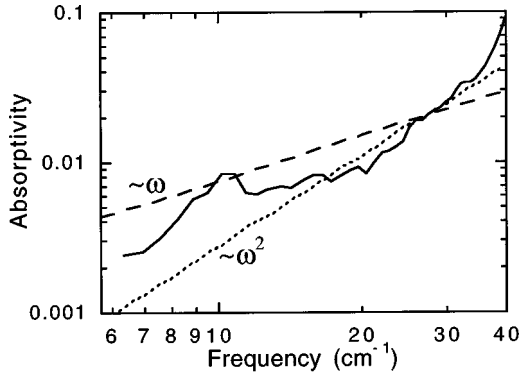


FIG. 5. Absorptivity at 2 K along the  $c$  axis of a  $\text{La}_{1.87}\text{Sr}_{0.13}\text{CuO}_4$  crystal. The dotted line is the best square law fit ( $A^c \propto \omega^2$ ) between 12 and  $35 \text{ cm}^{-1}$ , while the dashed line is the best linear fit ( $A^c \propto \omega$ ).

quency, occurs at a frequency  $1\text{--}2 \text{ cm}^{-1}$  higher in the absorptivity measurements at 2 K than in the ellipsometric data<sup>12</sup> at 10 K on the same sample. This may indicate that additional carriers are added to the condensate upon cooling the material from 10 to 2 K. The position of the reflectivity minimum is comparable to that found in the ellipsometric data.<sup>12</sup> The shapes of the curves above the minima are slightly different but consistent within the uncertainty of the measurements. Below the plasma edge, the reflectivity remains smaller than 100%, rising from 91% at  $40 \text{ cm}^{-1}$  to more than 99% at  $15 \text{ cm}^{-1}$ .

The absorptivity below  $40 \text{ cm}^{-1}$  is replotted in Fig. 5 on logarithmic axes. It drops rapidly with decreasing frequency until approximately  $12 \text{ cm}^{-1}$ . Below this frequency it rises to a small peak or shoulder at  $10 \text{ cm}^{-1}$  and then falls at even lower frequencies. Although this structure is weak, it appears to be a real feature in the optical response of  $\text{La}_{1.87}\text{Sr}_{0.13}\text{CuO}_4$ , since it was reproduced in different experimental runs involving different optical path geometries and filtering. The dotted and dashed lines are fits of the absorptivity between 12 and  $35 \text{ cm}^{-1}$  to square-law ( $A^c \propto \omega^2$ ) and linear ( $A^c \propto \omega$ ) dependences. The linear correlation coefficients of the fits are 0.98 and 0.85, respectively.

#### IV. KRAMERS-KRONIG ANALYSIS

We use the Kramers-Kronig (KK) relations in conjunction with our data from Fig. 2 to determine the complex dielectric function and the complex conductivity of  $\text{La}_{1.87}\text{Sr}_{0.13}\text{CuO}_4$ . Since we have measured the absorptivity over a finite frequency range, we must incorporate reflectivity data from other measurements as well as low and high frequency extrapolations. This is the standard procedure when using the KK relations. Our low-frequency extrapolation assumes that the reflectivity is unity below  $5 \text{ cm}^{-1}$ . The high-frequency extrapolation contains data<sup>11</sup> from reflectivity measurements ( $490 < \omega < 15\,000 \text{ cm}^{-1}$ ), a model function<sup>11</sup> for the interband transitions ( $15\,000 < \omega < 10^6 \text{ cm}^{-1}$ ) and a free-electron response above. Within the frequency range of the absorptivity measurements we have replaced our absorptivity data by reflectivity data<sup>11</sup> in the region ( $60 < \omega < 220 \text{ cm}^{-1}$ ) where the absorptivity is high and hence less reliable than reflectivity data, as discussed in conjunction with Fig. 3. We

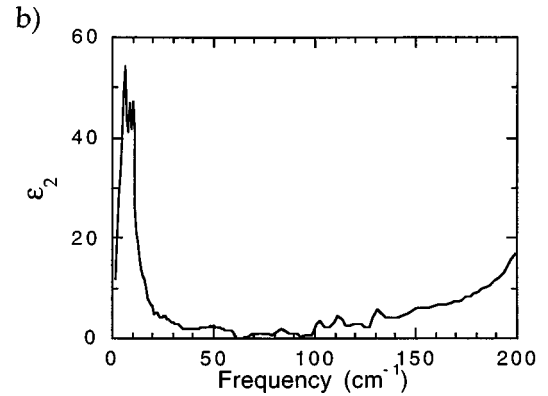
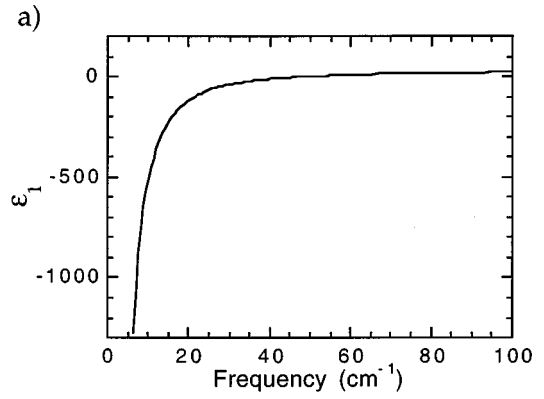


FIG. 6. Real (a) and imaginary (b) parts of the  $c$ -axis dielectric function of a  $\text{La}_{1.87}\text{Sr}_{0.13}\text{CuO}_4$  crystal at 2 K deduced from the Kramers-Kronig analysis.

have retained the absorptivity maximum from our experimental data, in spite of the uncertainty in the absolute value, since we want to investigate the position of the plasma edge at low temperature.

We compute the phase function  $\theta(\omega)$  using the Kramers-Kronig relation

$$\theta^c(\omega) = \frac{\omega}{\pi} \int_0^\infty \frac{\ln R^c(\omega') - \ln R^c(\omega)}{\omega^2 - \omega'^2} d\omega'. \quad (3)$$

In this manner we recover the phase information that is lost in the absorptivity measurement. From  $R^c(\omega)$  and  $\theta^c(\omega)$ , we compute  $\varepsilon^c(\omega)$  and  $\sigma^c(\omega)$ . We show the calculated real and imaginary parts of the complex dielectric function in Fig. 6. Numerical simulation shows that the results are insensitive to the low-frequency extrapolation used. Below  $10 \text{ cm}^{-1}$ , where  $R^c(\omega)$  is above 0.99, the uncertainty in  $R^c(\omega)$  rather than the extrapolation dominates the uncertainty in  $\theta^c(\omega)$  and hence in  $\varepsilon^c(\omega)$  and  $\sigma^c(\omega)$ . The details of the high-frequency extrapolation are somewhat more important as they add a small contribution to the conductivity that is roughly linearly dependent on frequency, but no reasonable extrapolation changes  $\varepsilon^c(\omega)$  or  $\sigma^c(\omega)$  qualitatively.

The  $\varepsilon_1^c(\omega)$  calculated using the KK analysis [Fig. 6(a)] is indistinguishable from that measured ellipsometrically for frequencies between 35 and  $100 \text{ cm}^{-1}$ . In Fig. 7 we plot the real part of the conductivity  $\sigma_1^c(\omega)$  for  $\omega < 160 \text{ cm}^{-1}$  calculated from the KK analysis to compare with the much noisier

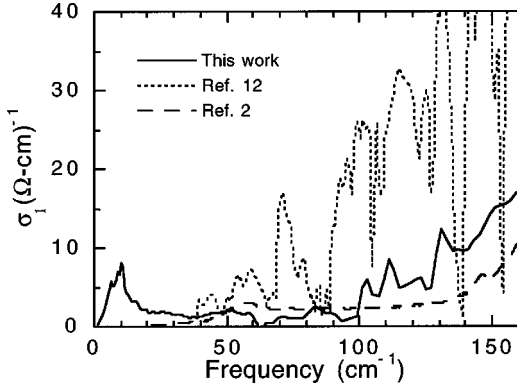


FIG. 7. Real part of the  $c$  axis conductivity at 2 K of a  $\text{La}_{1.87}\text{Sr}_{0.13}\text{CuO}_4$  crystal computed by Kramers-Kronig analysis as described in the text (solid curve), measured (Ref. 12) directly with ellipsometry on the same sample (dotted curve), and computed by Kramers-Kronig analysis of  $c$ -axis reflectivity data (Ref. 2) at 8 K for  $\text{La}_{1.84}\text{Sr}_{0.16}\text{CuO}_4$  (dashed curve).

ellipsometric measurement<sup>12</sup> of  $\sigma_1^c(\omega)$  made on the mosaic including our sample. We also plot  $\sigma_1^c(\omega)$  for a  $\text{La}_{1.84}\text{Sr}_{0.16}\text{CuO}_4$  crystal ( $T_c = 34$  K) calculated by KK analysis of reflectivity data<sup>2</sup> above  $25 \text{ cm}^{-1}$ . In this last data set, and also in our data, a small bump is seen in  $\sigma_1^c(\omega)$  near  $50 \text{ cm}^{-1}$ . This resonance has been discussed by Basov *et al.*,<sup>26</sup> but its significance remains unclear.

## V. DISCUSSION

It is clear from Fig. 5 that there is finite absorptivity along the  $c$  axis of  $\text{La}_{1.87}\text{Sr}_{0.13}\text{CuO}_4$  at least down to  $6 \text{ cm}^{-1}$ . The approximate  $\omega^2$  dependence of  $A^c(\omega)$  below  $35 \text{ cm}^{-1}$  suggests that a fraction of the carriers remains unpaired and can be described as a normal Drude liquid, even below 2 K. This loss may result from pair-breaking and thus suggests a strongly asymmetric superconducting gap with nodes, such as the  $d$ -wave gap which has been proposed and supported by microwave, NMR, magnetic, photoemission, and Josephson tunneling measurements.<sup>27</sup>

Following the two-fluid Gorter-Casimir model,<sup>28</sup> for the frequency range below the phonon transitions we write  $\varepsilon^c(\omega)$  as a sum of contributions from phonons, a superconducting London liquid with unscreened plasma frequency  $\omega_{ps}$ , and a normal Drude liquid with scattering rate  $\Gamma$  and plasma frequency  $\omega_{p0}$ :

$$\varepsilon^c(\omega) = \varepsilon_\infty - \frac{\omega_{ps}^2}{\omega^2} - \frac{\omega_{p0}^2 - \omega_{ps}^2}{\omega(\omega + i\Gamma)}. \quad (4)$$

In this model  $\omega_{ps}^2$  is proportional to the number of superconducting carriers, and  $\omega_{p0}^2 - \omega_{ps}^2$  is proportional to the number of unpaired carriers. As already mentioned, there is disagreement over the description of the normal state. It has been proposed both that the superconductivity is ‘‘clean’’ with  $\omega_{ps} \approx \omega_{p0}$  ( $\varepsilon_\infty = 20$ ,  $\omega_{p0} = 260 \text{ cm}^{-1}$ , and  $\Gamma = 120 \text{ cm}^{-1}$ )<sup>12</sup> and ‘‘dirty’’ with  $\omega_{ps} \ll \omega_{p0}$  ( $\varepsilon_\infty = 25$ ,  $\omega_{p0} = 1320 \text{ cm}^{-1}$ , and  $\Gamma = 4670 \text{ cm}^{-1}$ ).<sup>11</sup> Equation (4) can be inverted to solve for  $\omega_{ps}(\omega)$  in terms of  $\varepsilon^c(\omega)$ ,  $\varepsilon_\infty$ , and  $\omega_{p0}$ :

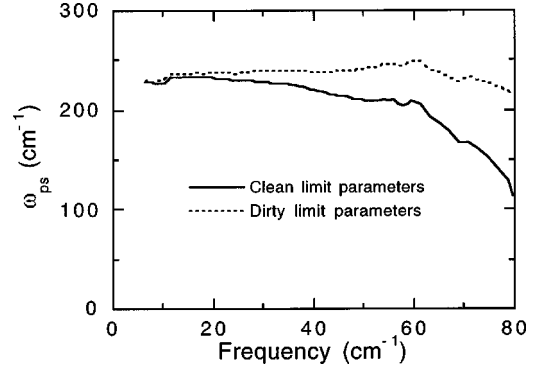


FIG. 8.  $\omega_{ps}(\omega)$  for a  $\text{La}_{1.87}\text{Sr}_{0.13}\text{CuO}_4$  crystal at 2 K computed from  $\varepsilon^c(\omega)$  using Eq. (5) for a clean limit (Ref. 12) (solid curve) and a dirty limit parametrization (Ref. 11) (dotted curve) of the normal fluid.

$$\omega_{ps}^2(\omega) = \omega^2 \left( \varepsilon_\infty - \varepsilon_1^c(\omega) + \frac{\varepsilon_2^c(\omega)^2 \omega^2}{\omega^2 [\varepsilon_\infty - \varepsilon_1^c(\omega)] - \omega_{p0}^2} \right). \quad (5)$$

In Fig. 8 we plot  $\omega_{ps}(\omega)$  for both the clean and dirty normal fluid descriptions. The extrapolation of  $\omega_{ps}(\omega)$  as  $\omega \rightarrow 0$  depends only weakly on the parametrization used and yields a value of  $\omega_{ps}$  of about  $230 \text{ cm}^{-1}$ . This measurement is consistent with the observed reflectivity edge which occurs at the screened plasma frequency  $\omega_p = \omega_{ps}/(\varepsilon_\infty)^{1/2}$ . The plasma frequency obtained with Eq. (5) from the ellipsometric measurements<sup>12</sup> on the same sample is  $260 \pm 40 \text{ cm}^{-1}$ .

The predictions for the frequency dependence of the conductivity in the superconducting state are qualitatively different for models assuming an isotropic  $s$ -wave or  $d$ -wave gap parameter. In the isotropic  $s$ -wave case, below the gap the conductivity drops rapidly towards zero with decreasing frequency. In the  $d$ -wave case the superconducting carrier pairs with zero or near zero binding energy are responsible for significant absorptivity as  $\omega \rightarrow 0$ . The addition of impurity scattering increases the low-frequency absorptivity for both the isotropic  $s$ -wave and the  $d$ -wave case. Carbotte *et al.* have considered the effects of impurity scattering and have argued<sup>29</sup> that the in-plane conductivity in  $\text{YBa}_2\text{Cu}_3\text{O}_{7-\delta}$  is more consistent with the  $d$ -wave prediction. We should keep in mind that it is not possible to distinguish between a  $d$ -wave gap of the  $k_x^2 - k_y^2$  variety and a strongly anisotropic  $|k_x^2 + k_y^2|$   $s$ -wave gap solely from measurements of the out-of-plane conductivity.<sup>30</sup> Our out-of-plane 214 results are consistent with calculations<sup>30,31</sup> for a gap with nodes; however, a detailed theoretical treatment is needed to rule out the possibility of impurity scattering.

While we cannot assign the absorptivity feature at  $10 \text{ cm}^{-1}$  to a specific excitation, we suggest that it may be related to the second plasmon resonance which appears<sup>15</sup> at temperatures just below  $T_c$  in very low-frequency ( $\sim 3 \text{ cm}^{-1}$ ) reflectivity measurements on 214 materials placed in large external magnetic fields. The resonance has not been studied at low temperatures. It has been proposed that this second mode is a longitudinal plasmon that is optically active due to finite sample size and magnetic excitation. Absorptivity measurements at a number of temperatures and magnetic field

strengths would be necessary to determine if the  $10\text{ cm}^{-1}$  feature corresponds to the same mode.

## VI. CONCLUSION

We have used bolometric direct absorption techniques to investigate the frequency- and temperature-dependent conductivity of a  $\text{La}_{1.87}\text{Sr}_{0.13}\text{CuO}_4$  single crystal at 2 K in the far-infrared region, down to approximately  $6\text{ cm}^{-1}$ , where the reflectivity is above 99%. A steep fall of reflectivity observed at approximately  $41\text{ cm}^{-1}$  is identified as the screened Josephson plasma frequency. This occurs at a frequency 1–2  $\text{cm}^{-1}$  higher than in the ellipsometric measurements<sup>12</sup> at 10 K made on the same sample. The difference suggests that additional carriers are added to the condensate upon cooling the material from 10 to 2 K. We have used a Kramers-Kronig analysis to compute the dielectric function  $\epsilon^c(\omega)$  and conductivity  $\sigma^c(\omega)$ . Our measurements of the  $\epsilon^c(\omega)$  give an unscreened plasma frequency  $\omega_{ps} = 230 \pm 10\text{ cm}^{-1}$ . This plasma mode is regarded as being of the Josephson type involving pair tunneling between  $\text{CuO}_2$  layers.<sup>3,10,32,33</sup> The existence of losses down to the low-frequency limit of our

absorptivity measurements ( $6\text{ cm}^{-1}$ ) is consistent with a gap with nodes, such as the  $k_x^2 - k_y^2$  *d*-wave gap model which enjoys nearly universal favor. Small peaks in the  $\sigma_1^c(\omega)$  have been detected at 10 and  $50\text{ cm}^{-1}$ . While we are not able to assign them to specific excitations, we note that the  $50\text{ cm}^{-1}$  structure has been observed previously,<sup>2,26</sup> and we suggest that the  $10\text{ cm}^{-1}$  structure may be related to a second Josephson plasmon resonance seen in reflectance measurements.<sup>15</sup>

## ACKNOWLEDGMENTS

This work was supported in part by the Director, Office of Energy Research, Office of Basic Energy Sciences, Materials Sciences Division of the U.S. Department of Energy under Contract No. DE-AC03-76SF00098. S.M.G. was supported by the Department of Education. A.W. acknowledges the support of a KBN grant under Project No. 2P03B7011. We thank A. Menovsky for growing the  $\text{La}_{1.87}\text{Sr}_{0.13}\text{CuO}_4$  crystal for us, D. van der Marel for useful discussions and sharing data in electronic format, and D. Miller for assistance with spectroscopy.

\*Author to whom correspondence should be addressed. Present address: Volen Center for Complex Systems, Brandeis University, Waltham, MA 02454.

†Present address: Jet Propulsion Laboratory, Mailstop 302-231, 4800 Oak Grove Drive, Pasadena, CA 91109.

‡Permanent address: Institute of Physics, Polish Academy of Sciences, Aleja Lotnikow 32, PL-02-668 Warszawa, Poland.

<sup>1</sup>P. W. Anderson, *Theory of Superconductivity in the High- $T_c$  Cuprates* (Princeton University Press, Princeton, 1997), and references therein.

<sup>2</sup>K. Tamasaku, Y. Nakamura, and S. Uchida, *Phys. Rev. Lett.* **69**, 1455 (1992).

<sup>3</sup>R. Henn, C. Bernhard, A. Wittlin, M. Cardona, and S. Uchida, *Thin Solid Films* **313–314**, 642 (1998).

<sup>4</sup>See special issue *J. Opt. Soc. Am. B* **6**, 283 (1989).

<sup>5</sup>U. Walter, M. S. Sherwin, A. Stacy, P. L. Richards, and A. Zettl, *Phys. Rev. B* **35**, 5327 (1987).

<sup>6</sup>P. E. Sulewski, A. J. Sievers, S. E. Russek, H. D. Hallen, D. K. Lathrop, and R. A. Buhrman, *Phys. Rev. B* **35**, 5330 (1987).

<sup>7</sup>Z. Schlesinger, R. L. Greene, J. G. Bednorz, and K. A. Müller, *Phys. Rev. B* **35**, 5334 (1987).

<sup>8</sup>D. A. Bonn, J. E. Greedan, C. V. Stager, T. Timusk, M. G. Doss, S. L. Herr, K. Kamarás, C. D. Porter, D. B. Tanner, J. M. Tarascon, W. R. McKinnon, and L. H. Greene, *Phys. Rev. B* **35**, 8843 (1987).

<sup>9</sup>Z. Schlesinger, R. T. Collins, M. W. Shafer, and E. M. Engler, *Phys. Rev. B* **36**, 5275 (1987).

<sup>10</sup>P. J. M. van Bentum, A. M. Gerrits, M. E. J. Boonman, A. Wittlin, V. H. M. Duijn, and A. A. Menovsky, *Physica B* **211**, 260 (1995).

<sup>11</sup>J. H. Kim, H. S. Somal, M. T. Czyzyk, D. van der Marel, A. Wittlin, A. M. Gerrits, V. H. M. Duijn, N. T. Hien, and A. A. Menovsky, *Physica C* **247**, 297 (1995).

<sup>12</sup>R. Henn, J. Kircher, M. Cardona, A. Wittlin, V. H. M. Duijn, and A. A. Menovsky, *Phys. Rev. B* **53**, 9353 (1996); R. Henn (private communication).

<sup>13</sup>Although there is no disagreement concerning the *position* of

phonon peaks, later ellipsometric studies (Ref. 32) of high quality 214 crystals grown in Tokyo demonstrated that the phonon linewidth and the oscillator strength depend significantly on the crystal quality. The superior crystals also showed a slightly lower overall electronic background conductivity than the nominally identical composition used in the present study.

<sup>14</sup>B. P. Gorshunov, A. V. Pronin, A. A. Volkov, H. S. Somal, D. van der Marel, B. J. Feenstra, Y. Jaccard, and J.-P. Locquet, *Physica B* **244**, 15 (1998).

<sup>15</sup>P. J. M. van Bentum, A. Wittlin, M. E. J. Boonman, M. Gross, S. Uchida, and K. Tamasaku, *Physica C* **293**, 136 (1997).

<sup>16</sup>J. T. Birmingham, S. M. Grannan, P. L. Richards, R. Henn, J. Kircher, M. Cardona, A. Wittlin, V. H. M. Duijn, and A. A. Menovsky, *Proc. SPIE* **2696**, 56 (1996).

<sup>17</sup>W. H. Weber, C. R. Peters, and E. M. Logothetis, *J. Opt. Soc. Am. B* **6**, 455 (1989).

<sup>18</sup>V. H. M. Duijn, N. T. Hien, A. A. Menovsky, and J. J. M. Franse, *Physica C* **235–240**, 559 (1994).

<sup>19</sup>N. S. Nishioka, P. L. Richards, and D. P. Woody, *Appl. Opt.* **17**, 1562 (1978).

<sup>20</sup>P. L. Richards, *J. Appl. Phys.* **76**, 1 (1994).

<sup>21</sup>D. Miller, P. L. Richards, S. Etemad, A. Inam, T. Venkatesan, B. Dutta, and X. D. Wu, *Phys. Rev. B* **47**, 8076 (1993).

<sup>22</sup>J. Bock, Thesis, U.C. Berkeley, 1994.

<sup>23</sup>E. I. DuPont de Nemours & Co., Wilmington, Delaware.

<sup>24</sup>W. A. Challener, P. L. Richards, S. C. Zilio, and H. L. Garvin, *Infrared Phys.* **20**, 215 (1980).

<sup>25</sup>E. E. Haller, N. P. Palaio, M. Rodder, W. L. Hansen, and E. Kreysa, in *Neutron Transmutation Doping of Semiconductor Materials*, edited by R. D. Larrabee (Plenum, New York, 1984), p. 21.

<sup>26</sup>D. N. Basov, H. A. Mook, B. Dabrowski, and T. Timusk, *Phys. Rev. B* **52**, 13 141 (1995).

<sup>27</sup>D. J. Scalapino, *Phys. Rep.* **250**, 331 (1995), and references therein.

<sup>28</sup>D. van der Marel, H. U. Habermeier, D. Heitmann, W. König, and A. Wittlin, *Physica C* **176**, 1 (1991).

- <sup>29</sup>J. P. Carbotte, C. Jiang, D. N. Basov, and T. Timusk, Phys. Rev. B **51**, 11 798 (1995).
- <sup>30</sup>M. Palumbo and J. J. Graf, Phys. Rev. B **53**, 2261 (1996).
- <sup>31</sup>P. J. Hirschfeld, S. M. Quinlan, and D. J. Scalapino Phys. Rev. B **55**, 12 742 (1997).
- <sup>32</sup>R. Henn, A. Wittlin, M. Cardona, and S. Uchida, Phys. Rev. B **56**, 6295 (1997).
- <sup>33</sup>V. Ambegaokar and A. Baratoff, Phys. Rev. Lett. **10**, 486 (1963); **11**, 104(E) (1963).